



**HAL**  
open science

# Representation of Laser Diffraction Diameter Distribution with a 3-Parameter Generalized-Gamma Function

Christophe Dumouchel, Jean-Bernard Blaisot, Viet-Dung Ngo

► **To cite this version:**

Christophe Dumouchel, Jean-Bernard Blaisot, Viet-Dung Ngo. Representation of Laser Diffraction Diameter Distribution with a 3-Parameter Generalized-Gamma Function. International Conference on Liquid Atomization and Spray Systems, Sep 2012, Heidelberg, Germany. hal-01649811

**HAL Id: hal-01649811**

**<https://normandie-univ.hal.science/hal-01649811>**

Submitted on 15 Feb 2023

**HAL** is a multi-disciplinary open access archive for the deposit and dissemination of scientific research documents, whether they are published or not. The documents may come from teaching and research institutions in France or abroad, or from public or private research centers.

L'archive ouverte pluridisciplinaire **HAL**, est destinée au dépôt et à la diffusion de documents scientifiques de niveau recherche, publiés ou non, émanant des établissements d'enseignement et de recherche français ou étrangers, des laboratoires publics ou privés.

## Representation of Laser Diffraction Diameter Distribution with a 3-Parameter Generalized-Gamma Function

C. Dumouchel\*, J.-B. Blaisot, V.D. Ngo  
CNRS UMR 6614 – CORIA, Université et INSA de Rouen, France  
name@coria.fr

### Abstract

The problem of the mathematical representation of liquid spray drop-size distribution has not been fully answered and is still debated in the literature. The present work participates to this debate by investigating the adequacy between the 3-parameter Generalized-Gamma function and the Laser Diffraction Technique (LDT) spray drop-size distribution. It is first pointed out that the 3-parameter Generalized-Gamma function and LDT distributions report similar properties. These similarities plead to the necessity of considering three parameters to reproduce LDT distribution. On this basis, a protocol to determine the three parameters is suggested and tested on experimental distributions measured for this purpose. In order to have the information concerning the actual small drop population, an Image Analyzing Technique (IAT) is used in complement to the LDT. The results show that the mathematical function reproduces very well the whole LDT drop-diameter distribution, its fractal characteristic and the mean-diameter series. Above this, these results were free of any parameter instability problem and the three parameters of the mathematical function display a clear relationship with the injection pressure. This work allows approaching a physical interpretation of the mathematical parameters in this situation. One of them characterizes the actual small drop population and the two others, the rest of the population as well as average information on the deviation from sphericity of the spray elements. These results reveal interesting aspects of the LDT diagnostic that are presented.

---

### Introduction

The question of a universal mathematical function to represent spray drop-size distribution has been addressed for many years and the number of parameters such a function should include is still debated. The ability of a mathematical function to represent liquid spray drop-size distribution is quantified by exploring its capability of representing experimental data. Since experimental diagnostics are not sensible to the same spray characteristics, we have reasons to believe that the more appropriate mathematical function to represent experimental data depends on the diagnostic used. In the present paper, we investigate the adequacy between the 3-parameter Generalized-Gamma function and Laser Diffraction Technique (LDT) distribution. The objective is to investigate the appropriateness of the 3-parameter Generalized Gamma function to represent LDT distribution and to propose and test a protocol to determine the parameters.

The 3-parameter Generalized-Gamma function has been established by a Maximum Entropy Formalism model [1]. This distribution is mathematically identical to the empirical Nukiyama-Tanasawa distribution that has been identified as very competent to reproduce measurement data [2]. However, parameter instabilities that manifests by a drastic change of their values for reasonable changes in operating condition have been reported and question the relevance of the three parameters. This point is addressed here.

The LDT is a commonly used laser-based technique to measure spray drop-diameter distributions [3, 4]. One of particularity of this technique is that it measures drops of any shape that goes through the instrument optical probe. Thus, the resulting drop-diameter distribution characterizes an equivalent system made of spherical elements [4]: it is the volume-based drop-diameter distribution of a set of spherical droplets that would produce the same diffraction pattern as the one recorded. Several investigations reported that this distribution is dependent on the shape of the droplets [5, 6]. This aspect of the instrument is taken into account in the present work by conducting an experimental work that cumulates two diagnostics to characterize liquid spray: LDT and an Image Analyzing Technique (IAT).

### The 3-Parameter Generalized-Gamma Function

The notations adopted throughout this paper are as follows.  $F(D)$  expresses a cumulative distribution of droplets with a diameter less than  $D$  and the distribution  $f(D)$  is the first derivative of this cumulative. Furthermore, the cumulative and distribution have a subscript  $n$  that indicates the description order:  $n = 0$  designates the

---

\* Corresponding author: Christophe.Dumouchel@coria.fr

number-based distribution;  $n = 1$  the length-based distribution,  $n = 2$  the surface-based distribution and  $n = 3$  the volume-based distribution. The general  $n$ -order expression of the 3-parameter Generalized-Gamma function is:

$$f_n(D) = \frac{dF_n(D)}{dD} = \frac{q}{\Gamma\left(\frac{\alpha+n}{q}\right)} \left(\frac{\alpha}{q}\right)^{\frac{\alpha+n}{q}} \frac{D^{\alpha+n-1}}{D_{q0}^{\alpha+n}} \exp\left(-\frac{\alpha}{q}\left(\frac{D}{D_{q0}}\right)^q\right) \quad (1)$$

where  $\Gamma$  is the Gamma function and  $q$ ,  $\alpha$  and  $D_{q0}$  are the three parameters. The two first parameters have no dimension and the last one is a mean-diameter of the series standardized by Mugele and Evans [1]. Despite the fact that  $q$  and  $\alpha$  can be either positive or negative provided they have the same sign [8], only positive parameters are considered in this work. One of the advantages of the 3-parameter Generalized-Gamma Distribution is that calculations can be performed [1]. In particular the mean-diameter series can be calculated:

$$D_{ab}^{a-b} = \left(\frac{q}{\alpha}\right)^{\frac{a-b}{q}} \frac{\Gamma\left(\frac{\alpha+a}{q}\right)}{\Gamma\left(\frac{\alpha+b}{q}\right)} D_{q0}^{a-b} \quad (2)$$

where  $a$  and  $b$  can take any real values provided that they are different. In the literature  $a + b$  is sometimes called the mean-diameter order. Being based on an exponential function, the distribution attributes extremely low frequencies to extremely large drops and imposes infinitely great maximum diameter, which is non-physical. In consequence the calculation of high-order mean-diameters with Eq. (2) is prohibited since they monotonously increase with the order. In real sprays, the infinite order mean-diameter tends toward the diameter of the biggest drop.

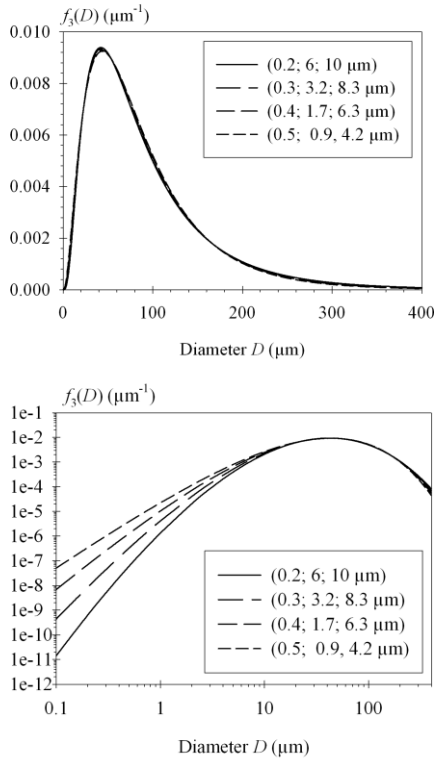


**Figure 1** Example of 3-parameter Generalized-Gamma function of different parameter triplets ( $q$ ;  $\alpha$ ;  $D_{q0}$ ) (Top: linear plot; Bottom: Log-Log plot)

The 3-parameter Generalized-Gamma function (Eq. (1)) is mathematically identical to the well-known Nukiyama-Tanasawa distribution and covers the Rosin-Rammler and the Weibull distributions [1]. These three empirical distributions have often been used in the literature to reproduce measurement data with sometimes a high degree of agreement. For instance, Paloposki [2] demonstrated that the Nukiyama-Tanasawa function is among the best to reproduce measurement data. Therefore, there is no doubt that the mathematical function given by Eq. (1) is competent in representing liquid spray drop diameter distribution in many different situations. (An illustration of this is available in [9].) A problem often reported when fitting measured data is the lack of stability of the parameters that manifests by a drastic variation of the parameters for reasonable changes in initial conditions. This can be illustrated by the fact that different parameter triplets can provide indiscernible distributions. This point is depicted in Fig. 1-top for a series of volume-based drop-diameter distributions  $f_3(D)$ . Such behaviour suggests that two parameters might be sufficient to provide an acceptable fit of the shape of the distribution. In other words, one may wonder whether we could take benefit of the presence of a third parameter to include another distribution characteristic in the fitting process.

The volume-based distributions shown in Fig. 1-top are reproduced in Fig. 1-bottom in a Log-Log plot. This representation reveals two important points: 1 – the distribution is proportional to a power of the diameter in the small diameter region; 2 – this dependency is a function of the parameters. The behaviour depicted in the small diameter region is observed for the cumulative as well as for the distribution whatever the order of description. It can be shown that in the small drop diameter region:

$$F_n(D) \propto D^{\delta+n} \quad \text{and} \quad f_n(D) \propto D^{\delta+n-1} \quad (3)$$

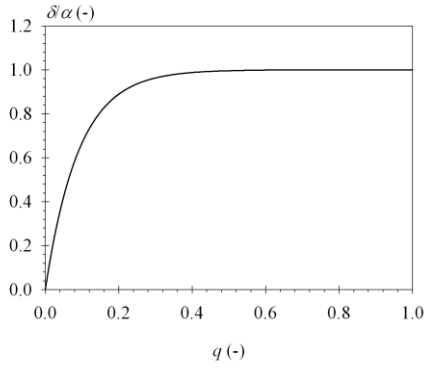


**Figure 2** The fractal dimension as a function of  $q$

Equation (4) is illustrated in Fig. 2. We note that when  $q$  is greater than 1, the fractal characteristic is equal to the parameter  $\alpha$ . This agrees with Eq. (1). In this situation, the parameter  $q$  controls the large diameter drop population only [1]. However, we see that when  $q$  is less than 1,  $\delta$  becomes a function of  $q$ , which therefore influences the small drop population also.

The results shown in Fig. 2 and in Eq. (4) reveal that different parameter triplets can report the same fractal characteristic. An example is presented in Fig. 3. However, this figure shows that despite the equality of the fractal dimension, the

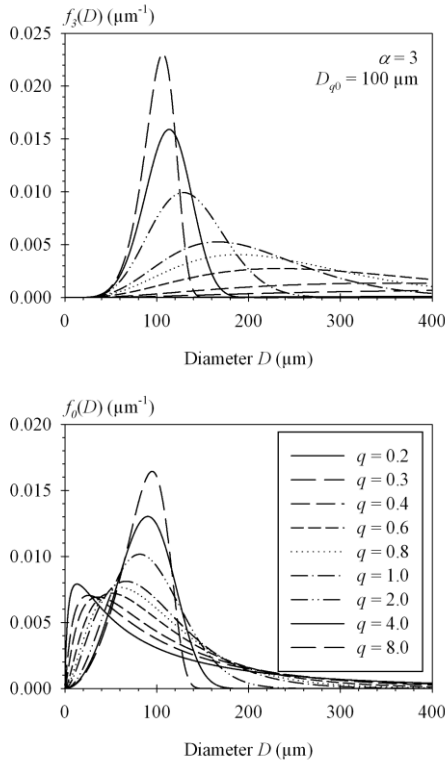


**Figure 4** Influence of the parameter  $q$  on the 3-parameter Generalized-Gamma distribution (Top: volume-based distribution  $f_3(D)$ ; Bottom: number-based distribution  $f_0(D)$ )

From a physical point of view, the dependency expressed by Eq. (3) has often been related to the self-similarity nature of fragmentation processes and therefore to the concept of fractal scaling [10-12]. On the other hand the fractal nature of liquid atomization processes has been experimentally reported [13, 14]. Therefore, the behaviour expressed by Eq. (3) in which  $\delta$  is a fractal dimension is physically relevant.

By examining Eq. (1), we note that the new function  $D_{q0} f_n(D/D_{q0})$  as a function of the new variable  $D/D_{q0}$  is independent of the mean diameter  $D_{q0}$ . Therefore, the fractal dimension  $\delta$  is independent of this parameter. A parametric investigation where  $q$  was varied from 0.1 to 1.4,  $\alpha$  from 2 to 6 and  $\delta$  was determined in the variable range  $D/D_{q0} \in [10^{-5}; 10^{-4}]$  reported the following relationships:

$$\frac{\delta}{\alpha} = 1 - \exp\left(-\frac{q}{0.091}\right) \quad (4)$$

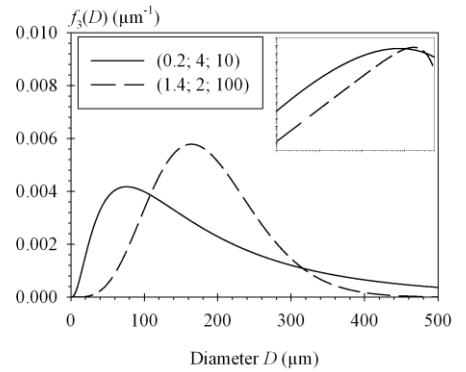


**Figure 3** Example of volume-based 3-parameter Generalized-Gamma distribution with identical fractal dimension (detail: Log-Log plot)

distributions are different. Therefore, the results in Figs. 1 and 3 demonstrate that the three parameters ensure independence between the shape of the distribution and the fractal characteristic. Of course two-parameter drop-diameter function would not report such a performance. For instance, the Rosin-Rammler distribution which is mathematically identical to Eq.(1) with  $\alpha = q - 3$  [1] has therefore a shape and a fractal dimension that both are imposed by the unique parameter  $q$ .

Equation (4) reproduced in Fig. 2 says that small  $q$  influence the fractal dimension. The influence of this parameter on the diameter distribution is shown in Fig. 4 (the two other parameters are kept constant, i.e.,  $\alpha = 3$ ;  $D_{q0} = 100 \mu\text{m}$ ). The top graph shows the volume-based drop-diameter distribution when  $q$  ranges from 0.2 to 8. As expected, we see that when  $q$  is great the distribution is stiff and as  $q$  decreases, the distribution spreads towards the large diameter population. As far as  $f_0(D)$  is concerned, we see that when  $q$  decreases, the maximum of the distribution first decreases and then increases whereas the peak diameter continuously decreases. We note that the distribution maximum is the smallest when the parameter  $q$  is of the order 0.4. This value is also the one under which the fractal dimension becomes dependent on  $q$  (see Fig. 2). Figure 4 illustrates to which extend small  $q$  influence

the drop population.

Finally, it can be seen that the above behaviour has repercussion on the mean-diameter series by calculating the mean-diameter ratio  $D_{m2}/D_{32}$  with the help of Eq. (2). This ratio that depends on the order  $m$  and on  $\alpha$  and  $q$  only, was calculated for a wide range of  $q$  and  $\alpha$  values, and for  $m$  maintained between 3 and 7, since, as explained above, high-order mean-diameters should not be calculated. For all calculations, the following relationship between the mean-diameter ratio and the order  $m$  was obtained:

$$\frac{D_{m2}}{D_{32}} = a'_2 m^2 + a'_1 m + a'_0 \quad (5)$$

The  $a'_2$  coefficient introduced in Eq. (5) is presented in Fig. 5. We see that when  $q > 0.8$ , Eq. (5) is linear and that it is a second order polynomial relationship otherwise. Thus, small values of  $q$  also change the dependence between the mean-diameter series and the mean-diameter order.

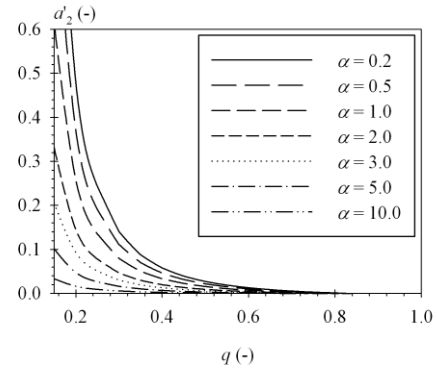


**Figure 5** Evolution of the parameter  $a'_2$  as a function of  $q$  and  $\alpha$

### Adequacy between LDT distribution and the 3-parameter Generalized-Gamma function and parameter determination

The question to be addressed here is whether the three parameters of mathematical function are necessary to reproduce LDT drop-diameter distribution. The answer can be approached by comparing LDT distribution and 3-parameter Generalized-Gamma function properties. A recent experimental work reported that LDT mean-drop diameter series followed a linear or a second order polynomial relationship with the mean diameter order [6]. As demonstrated in the previous section, the 3-parameter Generalized-Gamma allows reproducing such a characteristic thanks to the parameter  $q$ . Besides this, keeping the parameter  $\alpha$  ensures independence between the distribution shape and the fractal dimension, or, between the mean diameter series and the fractal dimension. Therefore, the three parameters should allow providing a better description than only two.

The question concerning the determination of the mathematical parameters is now addressed by considering the origin of the 3-parameter Generalized-Gamma function. This function has been established from a model based on the use of the Maximum Entropy Formalism (MEF) in which two constraints were written [1]. One of them ensures the existence of a maximum drop-diameter via the introduction of the parameters  $q$  and  $D_{q0}$ . The second constraint expresses the fact that diameter classes are not equally probable since the energy required to produce a given drop increases as its diameter decreases. Thus, a diameter-class probability distribution is imposed, limiting the production of small droplets. This second constraint introduced the parameter  $\alpha$  as the fractal dimension in the small drop-diameter range. In consequence, the analysis of this very population should return this parameter. The problem is that the LDT drop-diameter distribution depends on the shape of the droplets and characterizes an equivalent system of spherical drops that would produce the same diffraction pattern as the one recorded. As demonstrated by Mülhenweg and Hirlman [5], the variation of the shape of the elements modifies the whole equivalent LDT diameter distribution. Thus, the small drop population reported by LDT might not correspond to actual drops.

To overcome this problem, we suggest getting the information on actual small drops from a different diagnostic based on visualization and image analysis and to determine the value of the parameter  $\alpha$  on the actual small drop population. Once this parameter is determined, the two other parameters are determined as those ensuring the best fit of the LDT distribution. This protocol is tested in the second part of the paper.

### Experimental setup and Diagnostics

Water sprays produced by a single injector at several injection pressures are characterized. The injector used is a triple-disk injector whose description can be found elsewhere (Inj. 2 in [6]). It has a single cylindrical orifice whose diameter is equal to 400  $\mu\text{m}$ . The liquid flow issuing from this injector is a 2-dimension liquid sheet whose disintegration produces a rather 2-D spray. The injection pressure ranges from 0.2 MPa to 1 MPa and the injection is steady.

The Laser Diffraction Technique (LDT) equipment used in this work is the Spraytec 1997 from Malvern. It employs the Lorentz-Mie theory to calculate the drop-diameter distribution from the light diffraction pattern. The optical probe is a cylindrical laser beam with a wavelength equal to 670 nm and a diameter equal to 10 mm. The Spraytec is equipped with a 450 mm focal length collecting lens. This Fourier lens together with the 32 diodes of the receiver allows drop diameter ranging from 8.56  $\mu\text{m}$  to 1040.72  $\mu\text{m}$  to be measured. However, the parameters of the inversion code were determined in order to ensure a nice shape of the distribution in the small diame-

ter range with no undesirable secondary peaks. This was obtained by fixing a minimum diameter equal to 5  $\mu\text{m}$  to 12  $\mu\text{m}$  when the injection pressure decreases from 1 to 0.2 MPa. The adjustable sampling frequency of the instrument was set to 10 Hz and measurements were performed during 5 s. The drop-diameter distributions measured during this time interval were averaged. The center of the laser beam was positioned at 12 mm from the nozzle exit, distance at which the atomization process is completed for each operating condition as shown by the images described later. The transmission of the measurements, which is defined by the ratio of the non-deviated light intensity to the incident light intensity, was never less than 75%. According to experimental results reported on similar sprays [15], this value indicates negligible multiple-scattering effects. The optional light multiple-scattering algorithm is therefore not selected. The LDT reports a volume-based drop-diameter distribution  $f_3(D)$ . Using the traditional relationship between the diameter distribution of different orders, the corresponding surface-based drop-diameter distribution  $f_2(D)$  is calculated from

$$f_2(D) = \frac{D_{32}}{D} f_3(D) \quad (6)$$

Snapshots of the sprays are performed using a shadowgraph optical arrangement. The light source is a Nanolite from HSPS with a flash duration equal to 20 ns. In the present configuration, this light source plays the role of the shutter. The high resolution CCD camera is a DALSA (4016x2672 pixels) equipped with an objective that allows covering a physical field equal to 10.5 mm x 7.0 mm. This arrangement corresponds to a spatial resolution equal to 2.6  $\mu\text{m}/\text{pixel}$ . The centre of the image is located at 12 mm from the injector exit section. So LDT and Image Analysing Technique (IAT) cover almost the same portion of the spray.

The objective of the Image Analysing Technique is to provide supplementary information on the spray drop-size distribution in order to complete the LDT information. For this purpose, two points have to be addressed 1 – the drop characterisation; 2 – the drop selection. As far as the first point is concerned, we adopt here a classical approach that consists in characterizing each drop by the diameter of the circle that has the same area as the 2-D projection of the drop. Thus, being sensitive to the surface, the equivalent-diameters are used to build surface-based drop-diameter distributions  $f_2(D)$ . The drop selection is a tricky problem that has been considered with care in this work. IAT and LDT do not have the same measurement volume. LDT integrates all information along the optical axis ( $x$ -axis) whereas IAT considers sufficiently in-focus drops only. Thus, the two diagnostics do not perform the same spray sampling. This problem has been solved by performing a tomographic spray sampling thanks to a sophisticated technique developed in previous investigations [16, 17]. This technique allows the determination of the measurement volume, whatever the size of the drops, by the calibration of the Point Spread Function (PSF). For the present optical arrangement, the PSF calibration reported a measurement volume depth equal to 500  $\mu\text{m}$ . Then, considering the size, contrast and grey level gradient of any drop in the image, it is possible to know whether this drop belongs to the measurement volume and therefore whether it should be taken into account. By moving the spray along the optical axis ( $x$ -axis) with a step equal to the measurement volume depth, this protocol allowed performing a tomographic sampling of the spray and reconstructing a whole spray information from each slice.

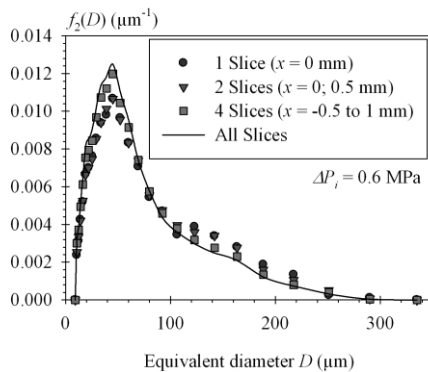


**Figure 7** Influence of the number of slices on the IAT surface-based drop-diameter distribution

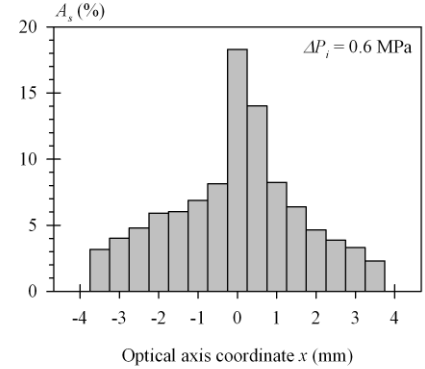


**Figure 6** Percentage of liquid surface in each spray slice

A preliminary test revealed that elements with an equivalent diameter less than 10  $\mu\text{m}$  were incorrectly measured. Therefore, these elements were disregarded. At each position of the measurement volume along the optical axis and for each injection pressure, the number of images taken and analysed was equal to 40. It was checked that the information cumulated from these 40 images was statistically representative.

At 0.6 MPa, the number of slices to cover the whole spray is equal to 15. This is shown in Fig. 6 which presents the percentage  $A_s$  of local liquid surface fraction, namely, local liquid surface area divided by total liquid surface area, as a function of the position  $x$  of the measurement volume on the optical axis. As expected, the slice under the injector ( $x = 0$ ) contains the greatest liquid proportion.

To lighten the experimental protocol and analysis, we evaluated the number of slices to be considered in order to ensure representative surface-based drop-diameter distributions. For the

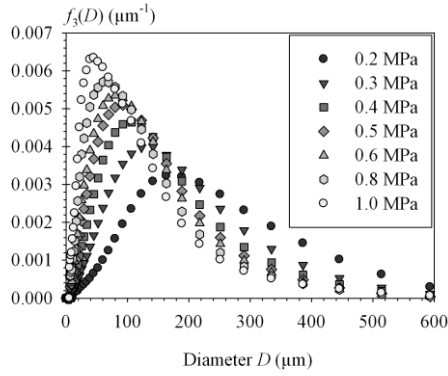


**Figure 8** LDT volume-based drop-diameter distribution (Influence of the injection pressure)

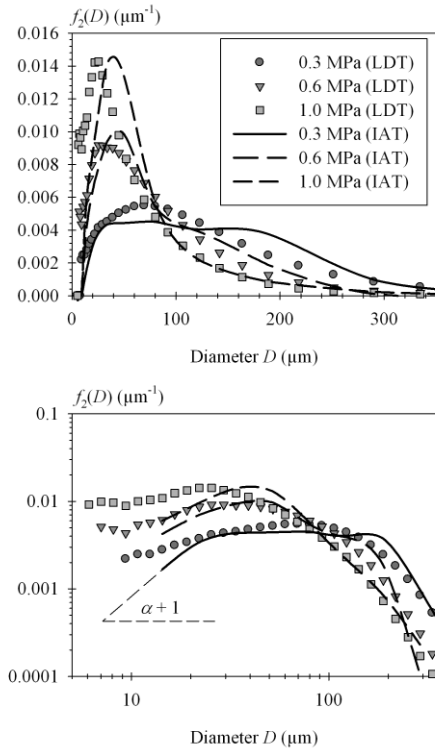


**Figure 9** Comparison between LDT and IAT surface-based drop-diameter distribution (top: linear scale; bottom: Log-Log scale)

tions are compared in a Log-Log scale. We see that the excess of small drops detected by LDT induces a decrease of the fractal dimension compared to the actual small drop population reported by IAT. Of course, we must keep in mind that the definition of the small drop population is dictated by the limitation of the experimental diagnostics. In the present work, the smallest detectable diameter for both diagnostics is of the order of 10  $\mu\text{m}$  and the diameter of the small drop population ranges from 10 to 30-40  $\mu\text{m}$  according to the injection pressure (see Fig. 9).

Following the MEF constraints from which the 3-parameter Generalized-Gamma function has been derived and that were men-

same situation as the one presented in Fig. 6, the results are shown in Fig. 7. This figure compares the surface-based drop-diameter distribution as a function of the considered spray slices. We see that when the four central slices are considered, the resulting surface-based drop-diameter distribution is identical to the one constructed with all slices. We note also that the distribution obtained with the central slice only is very close to the all-slice distribution. Therefore, we limited the measurement and analysis to the central slice only assuming that, for all injection pressures, it was sufficiently representative of the whole spray.

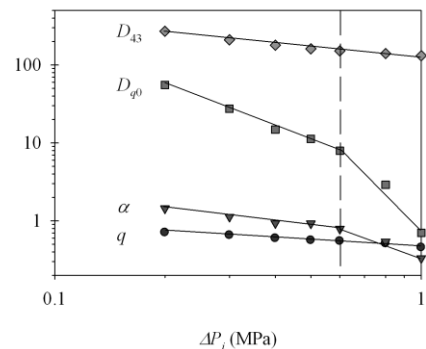
## Results and Applications

Figure 8 presents the LDT volume-based drop-diameter distribution. The traditional bell shape are seen. When the injection pressure increases, the modal diameter (diameter for which the distribution is maximum) decreases, the distribution maximum increases and the distribution tail collapses. This behaviour illustrates the increase of small particle production as the injection pressure increases.

As said above, LDT reports the volume-based drop-diameter distribution of the set of spherical elements that would produce the same diffraction pattern as the one recorded. This information depends on the shape of the particles [5]. To estimate the presence of non-spherical droplets, one compares the surface-based drop-diameter distributions corresponding to the LDT distributions with those obtained by IAT. This comparison is shown in Fig. 9 (Top graph) where LDT surface-based distribution is calculated from Eq. (6). If all droplets were perfectly spherical, and considering that both diagnostics perform an identical spray sampling as demonstrated in the previous section, LDT and IAT surface-based distributions should be the same. We see in Fig. 9 that this is not the case. Generally speaking, the small drop population is always greater with LDT than with IAT. This result says that the present spray contain non-spherical drops.

Non-spherical drops are always among the biggest elements and are characterized by great equivalent diameters. These diameters might be meaningless if the deviation from sphericity is great. On the opposite side of the diameter space, the small droplets are rather spherical and the IAT equivalent diameter is very near the actual diameter. Thus, the small drop population reported by IAT can be seen as a good estimation of the actual small-drop population.

The small drop population difference between the two diagnostics is clearer in the bottom graph of Fig. 9 where the distributions are compared in a Log-Log scale.



**Figure 10** Parameters and mean-diameter  $D_{43}$  of the mathematical distribution as a function of the injection pressure

tioned above, the parameter  $\alpha$  characterizes the actual small-drop population:  $\alpha$  is taken equal to the fractal dimension in the IAT small drop population and according to Eq. (3) is determined from the IAT surface-based drop-diameter distributions as indicated in Fig. 9-bottom. The parameters  $\alpha$  obtained this way are shown in Fig. 10 as a function of the injection pressure. The interesting aspect of these results is that the parameter  $\alpha$  shows a clear dependency with the injection pressure and no parameter instability is reported. Using these  $\alpha$  parameters, the two other parameters ( $q$  and  $D_{q0}$ ) ensuring the best fit with the LDT volume-based drop-diameter distributions have been determined. This was achieved via a  $\chi^2$  technique that consists in minimizing the “distance” between the measured and the mathematical distributions. This minimization was performed with the software Scilab. The resulting parameters  $q$  and  $D_{q0}$  are presented in Fig. 10 also. Note, as for the parameter  $\alpha$ , the clear evolution of these parameters with the injection pressure and the total absence of any parameter instability.

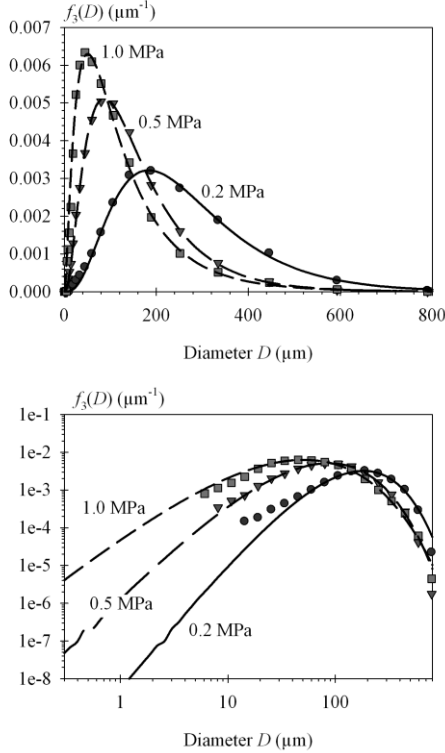


**Figure 11** Comparison between the LDT (dots) and the 3-parameter Generalized-Gamma (lines) volume-based drop-diameter distributions

reproduced by the mathematical function. Remembering that the fractal properties of LDT and IAT distributions are different (Fig. 9) and that the mathematical function fractal dimension depends on  $\alpha$  and  $q$  only (Eq. (4)), we conclude that this agreement is due to an adjustment of the parameter  $q$ .

As far as the mean-diameter series is concerned, a good agreement between experimental and calculated results is obtained (Fig. 12). In complement, Fig. 13 shows that the experimental and mathematical evolutions of the mean-diameter ratio  $D_{m2}/D_{32}$  as a function of the order  $m$  well agree also. The most interesting behaviour concerns the general evolution of the series. We see that both measured and calculated series report similar relationships with the order  $m$ : it is linear for low injection pressures and becomes a 2<sup>nd</sup> order polynomial dependence as the injection pressure increases.

We have demonstrated that the 3-parameter Generalized-Gamma function is well adapted to represent LDT drop-diameter distribution and that, when correctly chosen, the adjustable parameters are not unstable. In this investigation, the LDT diameter distribution characterizes an equivalent system of spherical elements since the actual droplets are not spherical. The parameter  $\alpha$  characterizes the actual small drop population. These droplets are spherical. On the other hand, the parameters  $D_{q0}$  and  $q$  control the rest of the population that might contain non-spherical elements. We therefore wonder whether the parameter  $q$  is sensitive to the lack of

Figure 10 shows that the decrease of the parameters of the Generalized-Gamma function with the injection pressure follows a power law. Whereas the power for the parameter  $q$  appears constant over the injection pressure range, the powers for the two other parameters decrease when the injection pressure becomes greater than 0.6 MPa. Although this specific behaviour has not been physically interpreted, it reveals a certain coherence of the parameter evolution with the injection pressure. The arithmetic mean of the mathematical volume-based drop-diameter distribution, i.e., the mean-diameter  $D_{43}$ , is plotted as a function of the injection pressure in Fig. 10. As often reported in the literature, we see that this mean-diameter decreases as the injection pressure increases following a power law. Note that, contrary to the parameters  $\alpha$  and  $D_{q0}$ , the power for  $D_{43}$  is constant over the investigated range of injection pressures.

The comparisons between the measured and the mathematical volume-based drop-diameter distributions are presented in Fig. 11. The top graph of this figure is a plot with linear scales and shows the results for three injection pressures. We note the very good agreement between the mathematical and the measured distributions. Such agreements have been obtained for the other injection pressures. The bottom graph of the same figure presents the same result in a Log-Log scale. We see that, besides the whole distribution shape, the behaviour in the small drop-population is very well

reproduced by the mathematical function. Remembering that the fractal properties of LDT and IAT distributions are different (Fig. 9) and that the mathematical function fractal dimension depends on  $\alpha$  and  $q$  only (Eq. (4)), we conclude that this agreement is due to an adjustment of the parameter  $q$ .

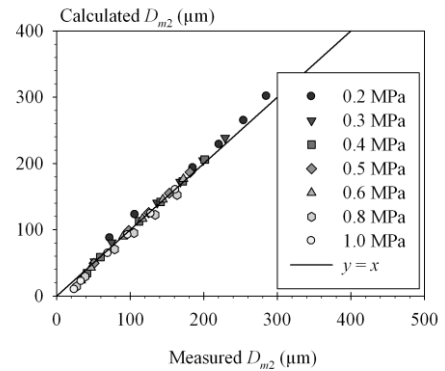


**Figure 12** Comparison of the measured and calculated mean-diameter series

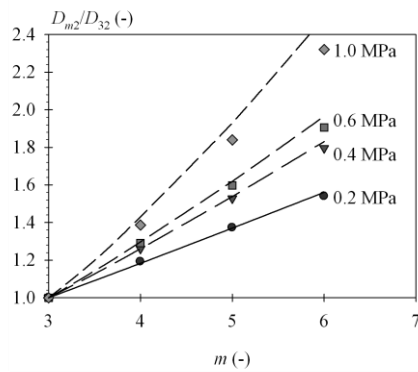


**Figure 13** Comparison of the mean-diameter ratio series (dots: measurements; lines: calculations)

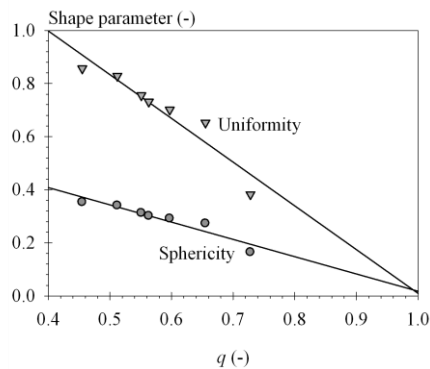


**Figure 14** Correlation between the  $q$  parameter and men shape parameters of the sprays

sphericity of the droplets. This point is investigated by measuring two shape parameters from the spray images, namely, the sphericity and the uniformity, and to calculate their averages for each operating conditions. These parameters defined in [16] are equal to 0 for spherical elements and increase when the deviation from sphericity is more and more pronounced. The sphericity parameter varies from 0 to 2 whereas the uniformity parameter varies from 0 to infinity. Figure 14 shows that the parameter  $q$  strongly correlates with these two shape parameters. The correlations indicate that the two shape parameters become equal to 0 when  $q = 1$ . This result says that values of  $q$  less than 1 corresponds to a set of non-spherical drops. In agreement with previous results [6], Fig. 5 indicates that in these situations, the LDT mean-diameter series shows a second order dependence with the mean-diameter order. This result also says that LDT drop-diameter distribution contains average information on the deviation from sphericity of the spray droplets.

### Discussion and Conclusions

As reported by other investigations ([2, 9] for instance), the results of this work confirm that the 3-parameter Generalized-Gamma function provides excellent reproduction of LDT volume-based drop-size distribution. Furthermore, this work proposes a protocol to determine the value of the adjustable parameters. Beside the LDT drop-diameter distribution, the results show that the 3-parameter Generalized-Gamma function provides a good representation of the fractal dimension of the distribution as well as of the mean-diameter series. Another interesting aspect of this result is that the adjustable parameters are not instable. Therefore, three parameters can provide a better representation of the measurement.

This work allows approaching a physical interpretation of the mathematical parameters when representing LDT drop-diameter distributions. The parameter  $\alpha$  qualifies the actual small-drop population, and is equal to the fractal characteristic of this population. The parameters  $D_{q0}$  and  $q$  qualify the rest of the population and  $q$  contains information on the lack of sphericity of the spray drops.

As far as the LDT technique is concerned we confirm that it is dependent on the shape of the droplets and learn that the presence of non-spherical droplets is interpreted as supplementary contribution in the small droplet range. Finally, thanks to the application of the mathematical function, we demonstrate that the LDT distributions contain average information on the lack of sphericity of the spray droplets. This conclusion agrees with those obtained in a previous investigation [6].

### References

- [1] Dumouchel, C., Part. Part. Syst. Charact. 23: 468-479 (2006)
- [2] Paloposki, T., *Drop-Size Distribution in Liquid Sprays*. Acta Polytechnica Scandinavica, Mechanical Engineering Series N° 114, Helsinki, Finland (1994)
- [3] Dodge, L.G., Rhodes, D.J., Reitz, R.D., Applied Optics 26: 2144-2154 (1987)
- [4] Black, D.L., McQuay, M.Q., Bonin, M.P., Prog. Energy Combust. Sci. 22: 267-306 (1996)
- [5] Mühlenweg, H., Hirleman, E.D., Part. Part. Syst. Charact. 15: 163-169 (1998)
- [6] Dumouchel, C., Grout, S., Leroux, B., Paubel, X., Part. Part. Syst. Charact. 27: 76-88 (2010)
- [7] Mugele, R.A., Evans, H.D., Ind. Engng. Chem. 43: 1317-1324 (1951)
- [8] Paloposki, T., Part. Part. Syst. Charact. 8: 287-293 (1991)
- [9] Lecompte, M., Dumouchel, C., Part. Part. Syst. Charact. 25 : 154-167 (2008)
- [10] Turcotte, D.L., Journ. Geophysical Research, 91: 1921-1926 (1986)
- [11] Tyler, S.W., Wheatcraft, S.W., Soil Sci. Soc. Am. J. 56: 362-369 (1992)
- [12] Brown, W.K., Wohletz, K.H., Journ. Appl. Physics. 78: 2758-2763 (1995)
- [13] Shavit, U., Chigier, N., Atom. Sprays 5: 525-543 (1995)
- [14] Grout, S., Dumouchel, C., Cousin, J., Nuglisch, H., IJMF 33: 1023-1044 (2007)
- [15] Triballier, K., Dumouchel, C., Cousin, J., Exp. In Fluids 35: 347-356 (2003)
- [16] Blaisot, J.B., Yon, J., Exp. In Fluids 39: 977-994 (2005)
- [17] Fdida, N., Blaisot, J.B., Meas. Scie. Techn., 21: 1-15 (2010)